Available online at www.sciencedirect.com
ScienceDirect
Journal of Power Sources 175 (2008) 732–738
JOURNAL OF POWER SOURCES
www.elsevier.com/locate/jpowsour

Estimation of flooding in PEMFC gas diffusion layer by differential pressure measurement

Kohei Ito [a,*], Kensuke Ashikaga [a], Hiromitsu Masuda [a], Toshihiro Oshima [a], Yasushi Kakimoto [b], Kazunari Sasaki [a]

[a] *Kyushu University, Faculty of Engineering, Department of Mechanical Engineering Science, Motooka 744, Nishi-ku, Fukuoka-shi, Fukuoka 819-0395, Japan*
[b] *Shizuoka University, 3-5-1 Joyous, Hamamatsu-shi, Shizuoka 432-8561, Japan*

Received 28 April 2007; received in revised form 1 October 2007; accepted 1 October 2007
Available online 13 October 2007

Abstract

The flooding, especially in gas diffusion layer (GDL), is one of the critical issues to put PEMFC to practical use. However, the experimental data of the flooding in GDL is so insufficient that the optimization design related to the water management for GDL has not established. In this study we developed a method to estimate the water saturation, namely the ratio of liquid water to pore volume in GDL. We fabricated a simple interdigitated cell where the supply gas is enforced to flow under rib. This structure enables to estimate the liquid water ratio in GDL by the measurement of differential pressure through the cell. We operated the cell and measured the differential pressure, and succeeded in estimating the water saturation, which changed largely with changing cell operation condition. In addition to this deferential pressure measurement, we measured the ionic resistance in polymer electrolyte membrane by ac impedance method. We evaluated and discussed the influence of the water saturation on cell voltage.

Keywords: Gas diffusion layer; Flooding; Water saturation; Differential pressure

1. Introduction

Water management is one of key issues to put PEMFC to practical use. When polymer electrolyte membrane (PEM) is not wet enough to have good ionic conductivity, the cell voltage decreases. So feed gases are humidified to prevent PEM from its dryness. On the other hand, flooding emerges in cell when the humidification of feed gases is excess. Once the flooding happens, it blocks gas supply to catalyst layer and makes cell voltage decrease or be in unstable, and then electricity generating will stop at worse case. Thus the water management is important issue, regarding the recent trend of high-current density operation and natural air breathing.

The flooding appears in every segment in cell, such as flow channel, gas diffusion layer (GDL) and catalyst layer. The flooding in flow channel is observed with visualization cell, in which its separator consists of transparent material [1–5]. On the other hand it is difficult to visualize the flooding in GDL and catalyst layer, because these layer has micro-porous structure and they are made with carbon material characterized as opaque material. The only way to observe the flooding in GDL is neutron-imaging technique, which is recently applied to the fuel cell research with large-scale equipment [6,7]. However, this technique seems to need further time and space resolution. Thus the adequate way to capture the flooding in GDL has not been established, and this situation invites insufficient understanding of the flooding in GDL.

Meanwhile the numerical simulation of flooding in PEMFC has been progressed. Based on the multiphase mixture model [8,9], a lot of two-phase flow simulation of PEMFC have been reported: a simulation which turns its attention especially to cathode channel and GDL [10], a simulation explicitly considering catalytic layer [11], a simulation focused on the GDL under

* Corresponding author. Tel.: +81 92 802 3144; fax: +81 92 802 0001.
E-mail addresses: kohei@mech.kyushu-u.ac.jp (K. Ito), masuda@mech.kyushu-u.ac.jp (H. Masuda), oshima@mech.kyushu-u.ac.jp (T. Oshima), sasaki@mech.kyushu-u.ac.jp (K. Sasaki).

0378-7753/$ – see front matter © 2007 Elsevier B.V. All rights reserved.
doi:10.1016/j.jpowsour.2007.10.019

Nomenclature

A_{GDL}	cross-section area of flow in GDL (m^2)
d_0	representative diameter of pore in GDL (m)
F	Faraday constant, 96485 ($C\,mol^{-1}$)
i_{mean}	mean current density ($A\,m^{-2}$)
K	permeability (Pa)
K_0	permeability of GDL itself (Pa)
L	rib length as shown in Fig. 1 (m)
n_i	number of electron related to anode/cathode reaction
P	pressure (Pa)
ΔP	differential pressure (Pa)
Q	flow rate specified with the standard temperature of 25 °C and the pressure of 0.101 MPa ($NL\,min^{-1}$)
R	gas constant, 8.3145 ($J\,mol^{-1}\,K^{-1}$)
s	water saturation
$S_{electrode}$	electrode area (m^2)
T	temperature (K)
v_D	Darcy velocity ($m\,s^{-1}$)

Greek symbols

ε	Porosity
η	gas utilization ratio
μ	viscosity (Pa s)

Superscripts

cloth	cloth GDL
paper	paper GDL

rib [12], a simulation for transient response of unit-cell [13]. In addition, there is a review article on fuel cell modeling [14].

These simulations have been evaluated by the comparison with the current–voltage characteristics measured. However, liquid water ratio to pore volume (water saturation), which can be obtained with two-phase flow simulation, has not been compared between simulation and experiment. Considering that the decrease of cell voltage is triggered by various physical phenomena, the precise evaluation of two-phase flow simulation of PEMFC needs a direct comparison with experiment data, such as the water saturation distribution.

On the basis of these backgrounds, we developed a method to observe the flooding in GDL implicitly. The water saturation, which corresponds to the extent of flooding, was estimated by the differential pressure between gas inlet and outlet of interdigitated cell, where the supplied gas is enforced to flow under rib [15]. This point, namely estimating the water saturation, is different from the previous studies: there the differential pressure through interdigitated cell was also measured, but the water saturation was not estimated [16,17].

Assuming that gases flow in GDL as Darcy flow and that the water droplet produced in GDL merely reduces its porosity, we estimate the water saturation from the differential pressure through interdigitated cell. At same time we measure the ionic

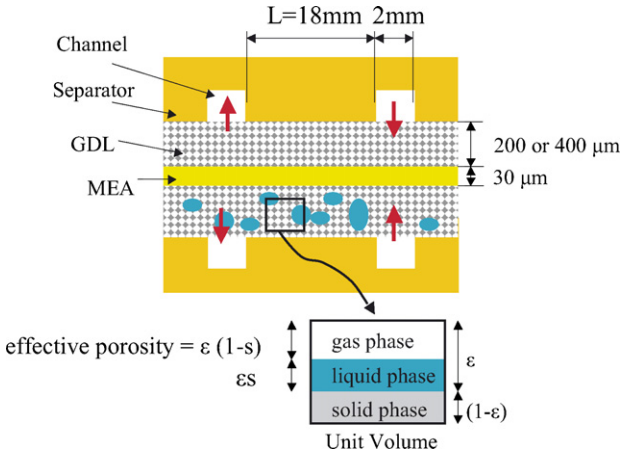

Fig. 1. Schema of cross-section of interdigitated cell and effective porosity denoted with water saturation of *s*.

resistance in PEM. By using both the water saturation and the ionic resistance, we discuss if flooding in GDL and/or drying in PEM cause the drop of cell voltage in high-current density region. Moreover we discuss the cyclic change of differential pressure and cell voltage under a supersaturated condition.

As just mentioned, we utilize a interdigitated cell for the estimation of water saturation. In the case of interdigitated cell, the representative velocity of gas in GDL is relatively fast. This fast velocity generates convection effect, which works as driving force to transport liquid water in GDL. Due to this convection effect, the water saturation in the case of interdigitated cell is thought to be smaller than that in the case of normal PEMFC where only capillary effect works as the driving force. Thus the magnitude of saturation value given by us is not applicable to normal PEMFC straightforwardly. However the dependency of the water saturation on operation condition, estimated by us, is available for PEMFC to some extent, and the estimated saturation value could contribute the evaluation of two-phase flow modeling.

2. Experimental method

The differential pressure through interdigitated cell is measured during electricity generating. When a water droplet forms in GDL, we can detect this event by the change of GDL permeability with the differential pressure measurement. In the followings we show how to determine the permeability of GDL itself, namely the permeability in the case that water droplets does not exist. Then we show how to estimate water saturation from the permeability given by the differential pressure when water droplets exist in GDL during electricity generating.

2.1. Permeability of GDL itself

With the interdigitated cell as shown in Fig. 1, the permeability of GDL itself, which is denoted as K_0, was measured. Differing from the typical interdigitated cell, the cell used here has simple structure: it has only one rib under which gas flows. This simple structure cell gives precise measurement for the dif-

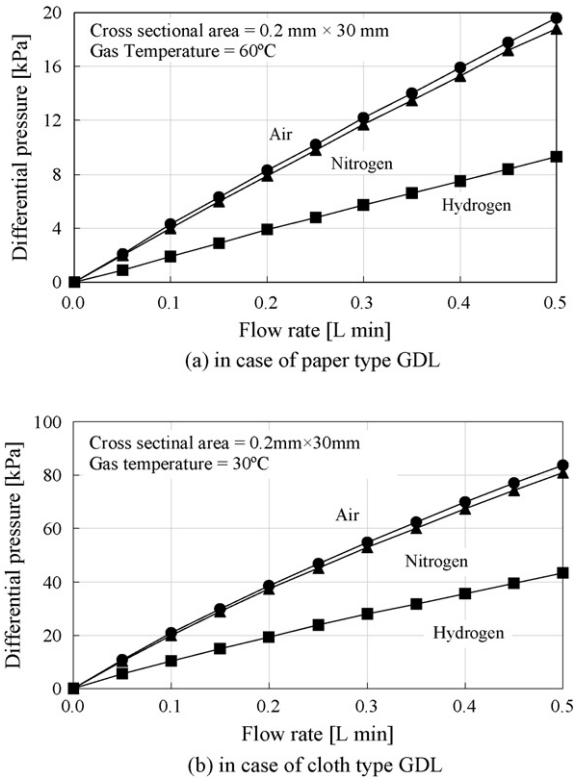

Fig. 2. Characteristic between flow rate and differential pressure through GDL.

ferential pressure caused by GDL, without considering parasitic pressure loss such as enlargement loss at flow branch.

Differential pressure gauge was positioned at the inlet and the outlet of the cell. The paper-type or cloth-type GDL, whose nominal thickness is 200 μm or 400 μm, was placed between separator and MEA as shown in the figure. As for the test gas to measure the permeability of GDL itself, nitrogen, hydrogen and dry air were chosen; each gas was supplied into the cell at various flow rates with mass flow controller. The cell temperature was maintained at 30 °C or 60 °C.

Fig. 2 shows the relationship between flow rate of Q and differential pressure of ΔP in case of paper- and cloth-type GDL. In both case, the ΔP increased in proportion to the Q. The permeability of K_0^{paper} and K_0^{cloth} can be given with this proportional relation and Darcy law denoted as

$$\Delta P = \frac{\mu}{K_0} v_D L \tag{1}$$

The permeability of K_0^{paper} and K_0^{cloth} obtained with this procedure is summarized in Table 1. Both the K_0^{paper} and K_0^{cloth} fluctuated within 3% with the change of gas species and cell temperature. From now on, we choose $K_0^{\text{paper}} = 2.71 \times 10^{-11}$ m^2 and $K_0^{\text{cloth}} = 5.45 \times 10^{-12}$ m^2 as the representative value of the permeability of GDL itself.

Table 1
GDL permeability estimated from differential pressure (unit: 10^{-11} m^2)

Type	Cell temperature	Air	N_2	H_2
Paper	30 °C	2.73	2.79	2.77
	60 °C	2.71	2.73	2.80
Cloth	30 °C	0.545	0.548	0.535

In addition to the permeability of GDL itself, the porosity and the pore diameter of GDL are also necessary to estimate the water saturation in GDL from differential pressure. The porosity $\varepsilon^{\text{cloth}}$ and $\varepsilon^{\text{paper}}$ were assumed to be 0.4 and 0.8. These values were obtained from Yoshizawa et al. [18], with the treatment that we compressed the carbon cloth by half. The representative diameter of d_0^{cloth} and d_0^{paper} were calculated to be 1.81×10^{-5} m and 6.78×10^{-5} m, which were derived with the assumption that the GDL has sphere-packed bed structure and satisfies the Blake–Kozeny equation [19]:

$$K_0 = \frac{\varepsilon^3}{150(1-\varepsilon)^2} d_0^2 \tag{2}$$

2.2. Estimation of flooding from differential pressure during generating electricity

For generating electricity, membrane electrode assembly (MEA) was inserted in this measurement. The thickness and the electrode area of MEA are 30 μm and 10 cm^2, respectively. The cell was operated with the test bench shown in Fig. 3. Hydrogen and air were supplied into anode and cathode, respectively. Before supplying gas into the cell, both the gases were humidified with bubbler. Current loaded to the cell was controlled with electronic load device (KIKUSUI, PLZ152A).

When the water droplet forms in GDL during cell operation, a portion of pores in GDL is occupied with liquid water denoted as a water saturation of s, and the effective porosity of GDL becomes $\varepsilon(1-s)$ as shown in Fig. 1. This effective porosity can be derived from the permeability measurement. The theoretical expression of the effective permeability, where pores in GDL is occupied with liquid water to some extent, is obtained by

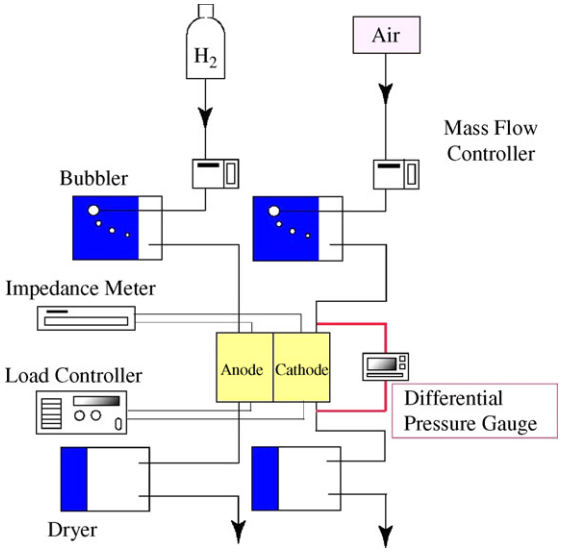

Fig. 3. Test bench for interdigitated cell. With this bench, ac impedance was also measured in addition to differential pressure.

substituting the effective porosity into Eq. (2):

$$K = \frac{\varepsilon^3(1-s)^3}{150\{1-\varepsilon(1-s)\}^2} d_0^2 \tag{3}$$

This effective permeability, denoted as K, becomes the permeability of GDL itself when s is equal to 0. Substituting Eq. (3) into Eq. (1) gives the relationship between differential pressure ΔP and water saturation s:

$$\Delta P = \frac{150\{1-\varepsilon(1-s)\}^2}{\varepsilon^3(1-s)^3 d_0^2} \mu v_D L \tag{4}$$

Thus the water saturation could be estimated from the differential pressure. To derive this equation, we used three assumptions: (1) the Blake–Kozeny equation is available, (2) water droplet spreads in GDL homogeneously and (3) the water droplet merely decreases the porosity of GDL. Although these assumptions should be evaluated quantitatively, we here accept noting that the reliable equation between porosity and permeability does not seem to be established for GDL, and that both 2nd and 3rd assumption can be accessible if current density is not so large.

The differential pressure through cathode GDL was measured, changing cell operation condition such as cell temperature, humidifier temperature, load current and gas flow rate. For specifying the representative Darcy flow rate v_D exactly, load current stopped in five second when the differential pressure data was acquired. The viscosity μ in Eq. (4) was given considering the mixture gas species in cathode: water vapor, nitrogen and oxygen gas.

The ionic resistance in PEM was also measured with ac impedance meter (Solatron, 1280Z). The meter was connected to the interdigitated cell, and small perturbation of ac current or voltage with a frequency was superimposed on dc load current. Then the complex impedance plot with changing frequency determined the ionic resistance in PEM.

3. Experimental results and discussion

In the Sections 3.1 and 3.2, we discuss the measurement result of cell voltage and water saturation under the steady condition. In the Section 3.3, we discuss in the case of forced-supersaturating condition, where the cell voltage and differential pressure could not be maintained to be constant.

In every measurement, the flow rate of supplied gas was regulated, and it was controlled with mass flow controller. The flow rate is indicated as hydrogen/oxygen utilization ratio of η_{H_2} and η_{O_2}. The gas utilization ratio is given with

$$\eta_i = \frac{Q}{6000} \frac{P_{STD}}{RT_{STD}} \frac{1}{i_{mean} S_{electrode}/(n_i F)} \tag{5}$$

The mean current density of i_{mean} is taken as 1 A cm^{-2} in this study. The n_i is 2 and 4 to hydrogen and oxygen gas, respectively. Other symbols are shown in the nomenclature.

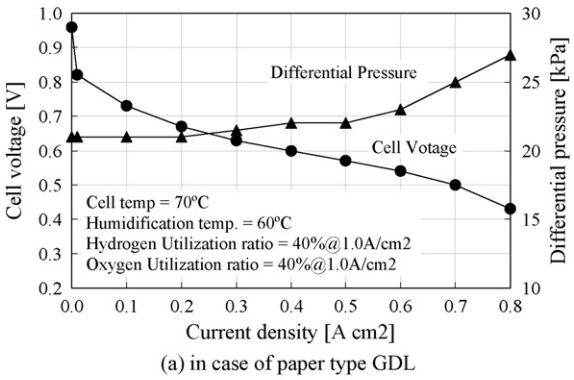

(a) in case of paper type GDL

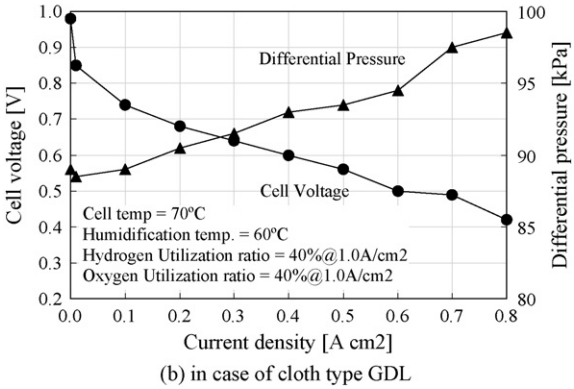

(b) in case of cloth type GDL

Fig. 4. Differential pressure and IV characteristic for interdigitated cell.

3.1. Change of cell voltage and water saturation with increasing load current

Fig. 4 shows the IV characteristic and the differential pressure under the condition: cell temperature $T_{cell} = 70\,^{\circ}C$ anode and cathode humidification temperature $T_{hum} = 60\,^{\circ}C$ hydrogen and oxygen utilization ratio $\eta = 40\%$ at 1 A cm^{-2}. Fig. 5 shows the water saturation estimated from Eq. (4) and the ionic resistance in PEM obtained by ac impedance method. In case of paper-type GDL the cell voltage decreased with the increase of load current especially when the load current was over 0.5 A cm^{-2}. The differential pressure was constant at about 21 kPa in the low-current density region, and increased in the region over 0.5 A cm^{-2}. In case of cloth-type GDL the cell voltage decreased and differential pressure monotonically increased with the increase of load current.

The water saturation estimated from the differential pressure also increased and reached 0.045 in case of paper, and 0.032 in case of cloth. This increase of water saturation is thought to be caused by the accumulation of produced water. On the other hand the ionic resistance showed small decline with the increase of load current. This is because the produced water wetted PEM. Therefore the relatively sudden decrease of cell voltage appeared over 0.5 A cm^{-2} in case of paper-type GDL (Fig. 4(a)) is considered to be caused by the concentration overvoltage triggered by the flooding in GDL.

The above discussion mentioned an evidence of concentration overvoltage even though the water saturation reached only 0.045 as shown in Fig. 5(a). This discussion is enforced by the

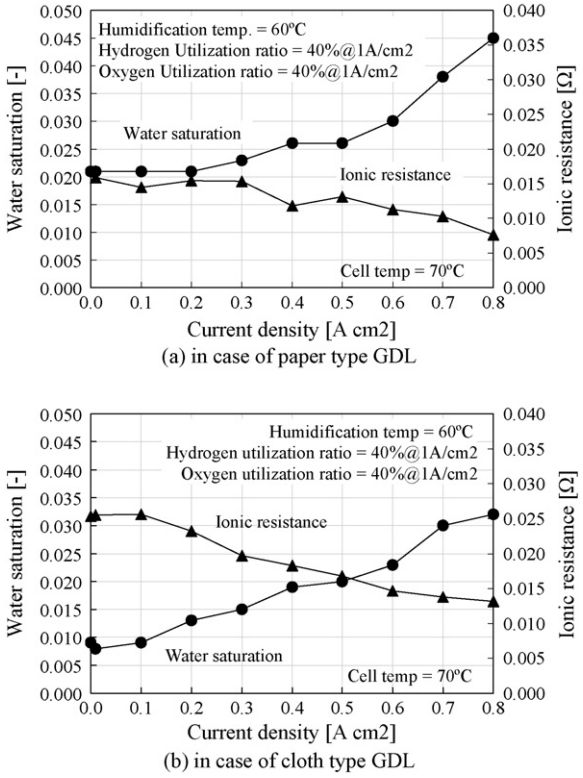

Fig. 5. Water saturation estimated and ionic resistance in PEM measured by ac impedance method.

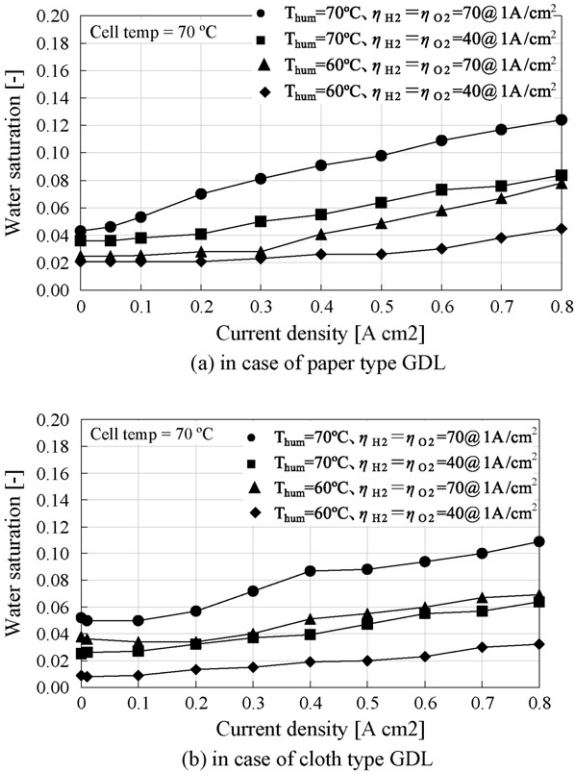

Fig. 6. Change of water saturation with the change of humidification temperatures and gas utilization ratio.

following consideration. As described in the measurement principle in the section of 2.2, the saturation obtained here means the value averaged to whole GDL. Practically the water saturation distributes in GDL, and the local water saturation near catalyst layer is larger than that in other location because of the water generation at the catalyst layer. This large saturation at the catalyst layer might cause the concentration overvoltage.

In general the drying-up in PEM at anode side also reduce cell voltage under high-current density operation. However, the concentration overvoltage caused by flooding was dominant factor to reduce cell voltage, within the experimental condition that the anode gas was supplied with sufficient humidification and this treatment kept PEM wet.

3.2. Change of water saturation with changing humidification temperature and gas utilization

Fig. 6 shows the water saturation under the condition: humidifier was controlled at 70 °C or 60 °C, gas utilization ratio was regulated at 70% or 40%, cell temperature was maintained as 70 °C. In any case the water saturation increased with increasing load current. Under the same utilization ratio the water saturation increased with increasing humidification temperature. It is considered that the higher humidification temperature promoted the condensation in GDL coupling to the water production by cell reaction, resulting in the higher water saturation. Under the same humidification temperature, the water saturation increased with increasing the utilization ratio. It is understood that higher utilization ratio (lower flow rate) degraded the drainage of water droplet in GDL, resulting in the higher water saturation. According to physical expectation, the water saturation changed with the change of cell operation condition. As shown in Fig. 6, the water saturation was not equal to 0 even when load current stopped. The reason why the water saturation was not equal to 0 might be caused by the unwilling supersaturation circumstance introduced by low accuracy of temperature control.

As a whole, Fig. 6 shows that the water saturation in the case of carbon-cloth GDL is rather smaller than that in the case of carbon-paper GDL. To discuss the reason, we show the general characteristic of the water transport in GDL briefly. The liquid water in GDL is driven by convection effect and by capillary effect. Considering our experimental condition that interdigitated cell was used and that the mass flow rate of gas supply to cell was regulated, the real gas velocity in GDL is fast, and convection effect becomes significant when the porosity and the pore diameter are small. The capillary effect depends on the hydrophobic property and the microscopic geometry in GDL. With these considerations, the following instinctive explanation is possible. The carbon-cloth GDL has smaller porosity and smaller pore diameter as described in Section 2.2, and it has larger convection effect under a regulated mass flow rate condition, leading to the smaller water saturation. We leave a discussion with involving the influence of the capillary effect, as for a future challenge.

The water saturation experimentally estimated by our study is compared to that obtained with numerical simulation study. As shown in Fig. 6 the maximum value estimated by us is about 0.12 under a saturated condition with the load current of 0.8 A cm^{-2}.

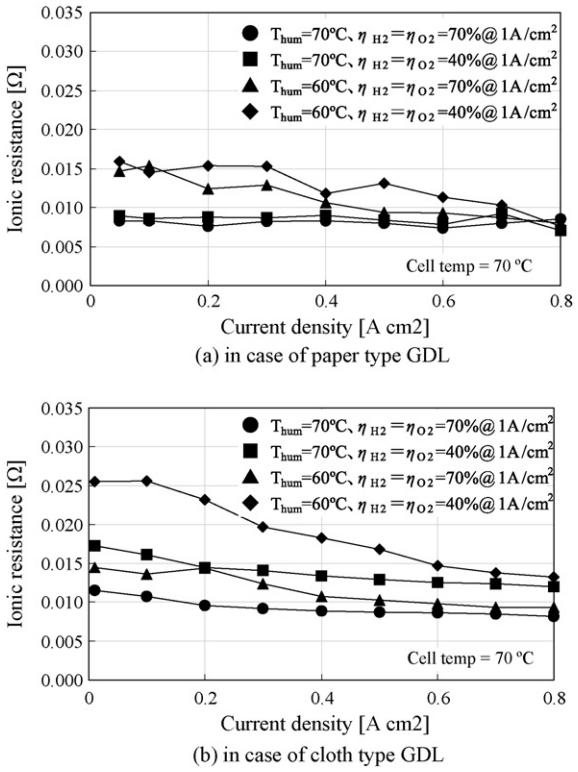

Fig. 7. Change of ionic resistance in PEM with the change of humidification temperatures and gas utilization ratio.

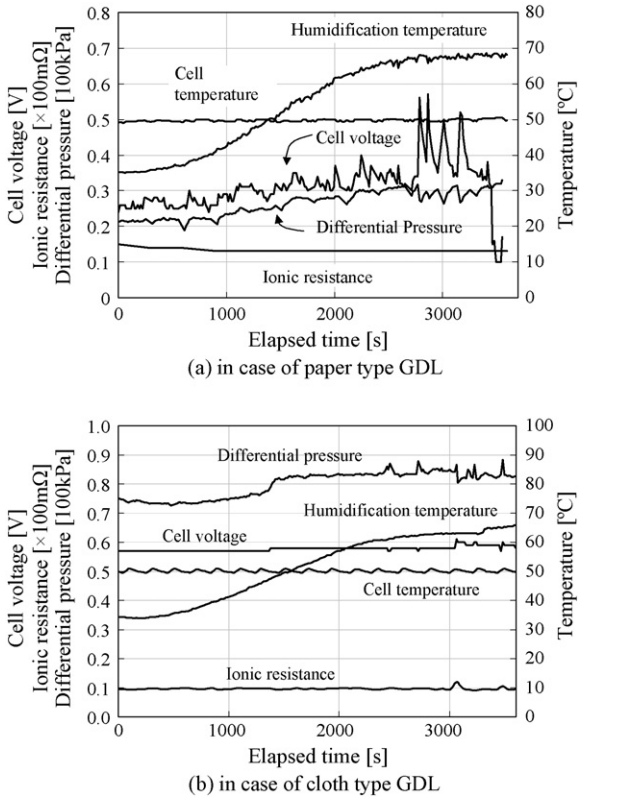

Fig. 8. Time evolutions of cell voltage, differential pressure and ionic resistance with successive increase of humidification temperature.

It is noted that the permeability used here is approximately from 10^{-12} m^2 to 10^{-11} m^2. Natarajan and Nguyen [20] numerically predicted water saturation of 0.9, which is larger than the value obtained by us. It is difficult to evaluate this discrepancy, because the cell geometry and the boundary condition, used in Natarajan and Nguyen simulation, is different from that used in our work. However, much smaller permeability of 10^{-14} m^2 applied in their study is a possible reason for this discrepancy. Pasaogullari and Wang [21] and Wang et al. [22] also numerically predicted water saturation of 0.1–0.2, which is approximately same as ours. The permeability used by them is 10^{-12} m^2, which is same digit as ours, leading to the comparable water saturation between their numerical study and our study.

Fig. 7 shows the ionic resistance in PEM. In the case of paper, the ionic resistance did not depend on load current under the humidification temperature of 70 °C, namely under the saturated condition, because the PEM was sufficiently wet without the water production by cell reaction. The ionic resistance decreased with increasing load current under the humidification temperature of 60 °C, because the produced water contributed to wet the PEM in this condition. Under the same humidification temperature, the lower the utilization ratio was, the larger the ionic resistance was. It is considered that the low-utilization ration (the high-flow rate) promotes the drainage of water in GDL resulting in drying PEM.

In the case of cloth, the ionic resistance changed as same as the case of paper. However the ionic resistance decreased with increase of load current even under the humidification temperature of 70 °C. Thus the ionic resistance change supports the characteristic that the drainage performance of cloth-type GDL is superior to that of paper-type GDL.

3.3. Cyclic change of cell voltage and differential pressure under forced-supersaturating condition

Fig. 8 shows cell voltage, differential pressure and ionic resistance when the humidification temperature is controlled as increasing from 35 °C to 70 °C successively. In this experiment, the other parameter of cell temperature, load current and utilization was kept as 50 °C, 0.6 A cm^{-2} and 42%, respectively. Increasing humidification temperature, the cell voltage and the differential pressure increased accompanying with small fluctuations. On the other hand the ionic resistance approximately constant.

In case of paper, at 2700s where the humidification temperature reached 70 °C, the cell voltage started to significantly fluctuate in about 100s cycle, roughly synchronizing with the differential pressure. This phenomenon is thought to be caused by the following mechanism; water droplet in GDL was periodically formed, accumulated and flushed when the pore of GDL filled with water; these successive events fluctuated the differential pressure; they also fluctuated the concentration overvoltage, resulting in the cyclic change of cell voltage. At 3400s the cell voltage decreased drastically, and electricity generation stopped. At this time the balance between the production and the removal of water might be broken, and gas supply might be blocked completely, leading to stopping the electricity generation.

In the case of cloth, both the cell voltage and the differential pressure did not oscillate significantly although the differential pressure increased. As mentioned in the previous section, the drainage performance of cloth-type GDL seems to be high comparing with paper-type GDL.

Thus, the differential pressure and the water saturation given by interdigitated cell correlates to cell voltage, well indicating how the flooding in GDL degrades the cell voltage. So the differential pressure can be one of the proper candidates for monitoring flooding in interdigitated cell. For future work, we will measure the differential pressure with changing the operation condition widely, and will extract the optimized operation condition where flooding is difficult to occur. Moreover we will apply the simple interdigitated cell used in this study to evaluate the reliability of two-phase flow PEMFC numerical simulation, because the simple geometry of this interdigitated cell, which can be characterized as two-dimensional structure, enables the rigorous comparison between experiment and simulation.

4. Summary

We operated a simple interdigitated cell and measured the differential pressure between inlet and outlet of the cathode. We estimated water saturation in paper or cloth-type GDL, obtaining the following:

(1) In the case of paper-type GDL, the change of slope at high-current density in IV characteristic was well explained in correlation with water saturation and concentration overvoltage.
(2) The water saturation increased with the increase of load current, gas utilization ratio and humidification temperature.
(3) When the humidification temperature was controlled as increasing successively to the supersaturated state, the cell voltage in case of paper-type GDL fluctuated largely in about 100s cycle, synchronizing with the differential pressure.
(4) The water drainage performance of cloth-type GDL is relatively high comparing with that of paper-type GDL in our condition.
(5) The differential pressure in interdigitated cell and the water saturation estimated from it are available for monitoring the flooding in GDL and for verifying the reliability of PEMFC numerical simulation.

Acknowledgement

This study was partially supported by the project "Research and Development of Polymer Electrolyte Fuel Cell" of New Energy and Industrial Technology Development Organization (NEDO), Japan.

References

[1] K. Tűber, D. Pócza, C. Hebling, Visualization of water buildup in the cathode of a transparent PEM fuel cell, J. Power Sources 124 (2003) 403–414.
[2] A. Hakenjos, H. Muenter, U. Wittstadt, C. Hebling, A PEM fuel cell for combined measurement of current and temperature distribution, and flow field flooding, J. Power Sources 131 (2004) 213–216.
[3] T. Ogawa, N. Nohara, K. Kikuta, T. Chikahisa, Y. Hishinuma, Observation of water production and temperature distribution in PEM fuel cell, in: Proceedings of the 41st National Heat Transfer Symposium of Japan, Toyama, 2004, pp. 235–236.
[4] X.G. Yang, F.Y. Zhang, A. Lubawy, C.Y. Wang, Visualization of liquid water transport in a PEFC, Electrochem. Solid State Lett. 7 (2004) A408–A411.
[5] F.Y. Zhang, X.G. Yang, C.Y. Wang, Liquid water removal from a polymer electrolyte fuel cell, J. Electrochem. Soc. 153 (2006) A225–A232.
[6] R. Satija, D.L. Jacobson, M. Arif, S.A. Werner, In situ neutron imaging technique for evaluation of water management system in operating PEM fuel cell, J. Power Sources 129 (2004) 238–245.
[7] D. Kramer, J. Zhang, R. Shimoi, E. Lehmann, A. Wokuan, K. Shinohara, G.G. Scherer, In situ diagnostic of two-phase flow phenomena in polymer electrolyte fuel cells by neutron imaging Part A. Experimental, data treatment, and quantification, Electrochem. Acta 50 (2005) 2603–2614.
[8] C.Y. Wang, P. Cheng, A multiphase mixture model for multiphase, multicomponent transport in capillary porous media 1. Model development, Int. J. Heat Mass Transfer 39 (1996) 3607–3618.
[9] P. Cheng, C.Y. Wang, A multiphase mixture model for multiphase, multicomponent transport in capillary porous media 2. Numerical simulation of the transport of organic com-pounds in the subsurface, Int. J. Heat Mass Transfer 39 (1996) 3619–3632.
[10] Z.H. Wang, C.Y. Wang, K.S. Chen, Two-phase flow and transport in the air cathode of proton exchange membrane fuel cell, J. Power Sources 94 (2001) 40–50.
[11] L. You, H. Liu, A two-phase flow and transport model for the cathode of PEM fuel cell, Int. J. Heat Mass Transfer 45 (2002) 2277–2287.
[12] M. Hu, A. Gu, M. Wang, X. Zhu, L. Yu, Three dimensional, two phase flow mathematical model for PEM fuel cell Part 1. Model development, Energy conversion and management 45 (2004) 1861–1882.
[13] K. Ito, H. Masuda, T. Miyazaki, Y. Kakimoto, T. Masuoka, Investigation of flooding phenomena in PEMFC by two-phase flow numerical simulation, in: Proceedings of the 3rd International Conference on Fuel Cell Science, Engineering and Technology, Yipsilanti, MI, USA, May 22–25, 2005.
[14] C.Y. Wang, Fundamental models for fuel cell engineering, Chem. Rev. 104 (2004) 4727–4766.
[15] D.L. Wood, Y.S. Yi, T.V. Nguyen, Effect of direct liquid water injection and interdigitated flow field on the performance of proton exchange membrane fuel cells, Electrochem. Acta 43 (1998) 3795–3809.
[16] W. He, G. Lin, T.V. Nguyen, Diagnostic tool to detect electrode flooding in proton-exchange-membrane fuel cell, AIChE J. 49 (2003) 3221–3228.
[17] H. Yamada, T. Hatanaka, Y. Morimoto, Evaluation of flooding in gas diffusion layer of PEFCs using pressure drop measurement, in: Proceedings of the 73th Annual Meeting of the Electrochemical Society of Japan, 2005, p. 214, Abstr.
[18] K. Yoshizawa, et al., Analysis of gas diffusion layer and flow field design in a fuel cell, in: The 13th FCDIC Fuel Cell Symposium Proceedings, Tokyo, Japan, May 16–17, 2006, pp. 238–241.
[19] R.B. Bird, W.E. Stewart, E.N. Lightfoot, Transport Phenomena, John Wiley & Sons Inc., 1960, p. 199.
[20] D. Natarajan, T. Nguyen, A two-dimensional, two-phase, multicomponent, transient model for the cathode of a proton exchange membrane fuel cell using conventional gas distributors, J. Electrochem. Soc. 148 (2001) A1324–A1335.
[21] U. Pasaogullari, C.Y. Wang, Two-phase modeling flooding prediction of polymer electrolyte fuel cells, J. Electrochem. Soc. 152 (2005) A380–A390.
[22] Y. Wang, C.Y. Wang, A nonisothermal two-phase model for polymer electrolyte fuel cells, J. Electrochem. Soc. 153 (2006) A1193–A1200.